ELSEVIER

Polymer 42 (2001) 501–513

polymer

www.elsevier.nl/locate/polymer

Testing models for penetrant diffusion in glassy polymers

M.P. Tonge, R.G. Gilbert*

Key Centre for Polymer Colloids, School of Chemistry, University of Sydney, Sydney, NSW 2006, Australia

Received 16 September 1999; received in revised form 10 March 2000; accepted 7 April 2000

Abstract

Data from forced-Rayleigh scattering studies of diffusion coefficients for camphorquinone and diacetyl in poly(methyl methacrylate) in the glassy regime were used to test two models for this quantity. Free-volume theory with the parameter-choice method suggested by Vrentas and co-workers [Vrentas JS, Vrentas CM. Eur Polym J 1998;34:797] predicts an activation energy (ca. 250 kJ mol^{-1}) which is a factor of about 2 greater than experiment, and a pre-exponential factor which is several orders of magnitude too large: thus this model underestimates experimental diffusion coefficients by many orders of magnitude at the temperatures studied. This is ascribed to free-volume theory being inapplicable to the actual mechanism for penetrant diffusion in glassy polymers: simulations suggest that this occurs instead by occasional jumps between cavities through the opening of a “neck”. This jump mechanism is explicitly taken into account by the second model tested here [Gray-Weale AA, Henchman RH, Gilbert RG, Greenfield ML, Theodorou DN. Macromolecules 1997;30:7296]. Although this model successfully predicts diffusion coefficients of small nonpolar penetrants, it is found to greatly overestimate observed diffusion coefficients in the present system, perhaps because it underestimates the attractive potentials between the penetrant and the polymer matrix and/or breakdown of the model’s assumption of linear elastic deformation for relatively large penetrants. © 2000 Elsevier Science Ltd. All rights reserved.

Keywords: Diffusion; Glassy polymers; Penetrant species

1. Introduction

A knowledge of diffusion coefficients of penetrant species in glassy polymers is useful in a number of different fields, including membrane separation [1], controlled-release technology [2], minimization of residual monomer in free-radical polymerization [2], the kinetics and molecular weight distribution in free radical polymerizations [2–4], and the development of composite particle morphology in polymer colloids [5–8]. Reliable experimental data for such diffusion coefficients are hard to obtain. There are a number of reasons for this difficulty, including the long time scales involved and the difficulty of sample preparation (including the possibility of ageing effects [9–11], and the possibility of non-Fickian—or “anomalous”—diffusion [12–14]).

Theory has an important part to play here: for example, if one could predict activation energies reliably, then it would be possible to extrapolate data obtained at one temperature to different temperatures. Theories may be subdivided into two categories (see [1] for a recent overview and references): simulations (here the transition-state simulation approach is particularly fruitful) and “molecular” theories such as the free-volume approach. While atomistic simulations offer the best hope of reliable prediction, such simulations require huge computational resources, and even then can (at present) only be applied to very simple penetrants. Molecular theories, particularly those which permit evaluation of diffusion coefficients with minimal computational resources and from readily available information, are therefore needed, both from the pragmatic viewpoint of data prediction or extrapolation and, perhaps more significantly, from the insight that may be gained into the mechanism of diffusion.

The present paper uses recent experimental data for the diffusion coefficients for two penetrants, camphorquinone and diacetyl, in glassy poly(methyl methacrylate), PMMA, with the saturated equivalent of monomer (methyl isobutyrate) as diluent [15]. Measurements were made at polymer weight fractions, w_p, over the range 0.78–0.90 and temperature range 25–50°C for camphorquinone (which spans the glass transition regime), and at $w_p = 0.90$ and 0.95 and at room temperature for diacetyl. Results for camphorquinone showed a strong temperature dependence, with diffusion coefficients changing as much as two orders of magnitude between 25 and 50°C, and showing high activation energies

---

* Corresponding author. Fax: +61-2-9351-8651.
E-mail address: gilbert@chem.usyd.edu.au (R.G. Gilbert).

0032-3861/01/$ - see front matter
PII: S0032-3861(00)00338-4

Table 1
Free-volume parameters used for the prediction of diffusion coefficients for camphorquinone in PMMA

Parameter	Value	Reference
$\hat{V}_2^*$ (cm^2 g^{-1})	0.788	[31]
K_{12}/γ (cm^3 g^{-1} K^{-1})	3.05×10^{-4}	[31]
$K_{22}-T_{g2}$ (K)	-301	[31]
T_{g2} (K)	388	[27]
α_2 (cm^3 g^{-1} K^{-1})	5.70×10^{-4}	[27]
$\hat{V}_2^0(T_{g2})$ (cm^3 g^{-1})	0.8489	[27]
α_{2g} (cm^3 g^{-1} K^{-1})	2.60×10^{-4}	[27]
δ_1 (cal$^{1/2}$ cm$^{-3/2}$)	10.5	See text
δ_2 (cal$^{1/2}$ cm$^{-3/2}$)	9.05	[20]
$\tilde{V}_2^*$ (cm^3 mol^{-1})	135	[16]
$\tilde{V}_1^0(0)$ (cm^3 mol^{-1})	185	[32]
$\bar{D}_0$ (cm^2 s^{-1})	2.74×10^{-3}	[33]
$(\bar{B}/\bar{A})^{-1}$	0.9	See text

for diffusion: $\sim$125 kJ mol^{-1}. Since these are ternary systems (consisting of tracer dye, diluent, and polymer), in the present paper comparisons are only made for the limit as w_p approaches 1, i.e. in the absence of diluent. The observed w_p-dependence of the measured diffusion coefficients above $w_p \sim 0.85$ was relatively small, enabling the data to be extrapolated to penetrant in pure polymer ($w_p = 1$). While these data are subject to considerable uncertainty, it will be seen that it is possible to make a meaningful assessment of the applicability of the models and/or parameters used therein. The two molecular theories used for this comparison are free-volume theory with the parameter-choice method suggested by Vrentas et al. [16], and the "typical jump" model of Gray-Weale et al. [17], (the latter being based upon precepts deduced from transition state simulations [1]). Each of these uses parameters that are readily available (such as bulk properties of the solid) and are easily evaluated.

2. Free-volume theory

Free-volume theory [18], in the formulation and parameters of Vrentas et al. [16], has been applied to diffusion coefficients in a glassy matrix. As stated, comparisons here are confined to the binary polymer-penetrant system, i.e. $w_p = 1$; an extension of free-volume theory to ternary systems (i.e. penetrant + polymer + diluent, corresponding to $w_p < 1$) has been made for rubbery systems [18,19], but would need further modification to predict diffusion coefficients for the current glassy system; this would lead to too many free variables, thus rendering any comparisons meaningless.

The Vrentas formulation calculates diffusion coefficients from the basic expression:

$$\ln D_1 = \ln \bar{D}_0 - \frac{E^*}{\mathrm{R}T} - \left\{ \frac{(1-\omega_2)\hat{V}_1^* + \xi\omega_2\hat{V}_2^*}{\hat{V}_{FH}/\gamma} \right\} \tag{1}$$

where D_1 is the diffusion coefficient, $\bar{D}_0$ is a constant, E^* the effective energy per mole that a molecule needs to overcome attractive forces, R the gas constant, T the temperature, ξ is the size parameter, $\hat{V}_1^*$ and $\hat{V}_2^*$ are the specific volumes of monomer and polymer, respectively, and $\hat{V}_{FH}$ is the average hole free volume per gram of mixture, γ is an average overlap value in the mixture, and $\omega_2 = w_p$. For $w_p = 1$ (which allows simpler expressions than in the presence of solvent), the free volume of the glassy polymer solution is calculated as follows:

$$\hat{V}_{FH}/\gamma = \hat{V}_{FH2g}/\gamma_2 \tag{2}$$

where

$$\hat{V}_{FH2g} = \hat{V}_2^0(T_{g2})[f_{H2}^G + (\alpha_{2g} - \alpha_{c2g})(T - T_{g2})] \tag{3}$$

Here $\hat{V}_2^0(T_{g2})$ is the specific volume of the polymer at T_{g2}, f_{H2}^G is the fractional hole volume of the polymer at T_{g2}, α_{2g} is the thermal expansion coefficient for the glassy polymer, α_{c2g} is the thermal expansion coefficient for the sum of the specific occupied volume and the specific interstitial free volume for the glassy polymer, T_{g2} is the glass transition temperature of the pure polymer, and γ_2 is the overlap factor for free volume of pure polymer. The parameters are calculated as follows:

$$f_{H2}^G = \alpha_2 K_{22};\quad \alpha_{c2} = [\ln(\hat{V}_2^0(T_{g2})(1 - f_{H2}^G)/\hat{V}_2^0(0))/T_{g2}];$$

$$\gamma_2 = [\hat{V}_2^0(T_{g2})\alpha_2]/\left(\frac{K_{12}}{\gamma_2}\right) \tag{4}$$

$$\hat{V}_2^* = \hat{V}_2^0(0);\quad \frac{\alpha_{c2g}}{\alpha_{c2}} = \left.\frac{\alpha_{2g}}{\alpha_2}\right|_{T=T_{g2}} \tag{5}$$

where K_{22} is one of the polymer free volume constants, α_{c2} is the thermal expansion coefficient for the sum of the specific occupied volume and the specific interstitial free volume for the equilibrium liquid polymer, $\hat{V}_2^0(0)$ is the specific volume of the equilibrium liquid polymer at 0 K, (K_{12}/γ_2) is a polymer free volume parameter, and α_2 is the thermal expansion coefficient of the equilibrium liquid polymer.

The value of ξ is estimated as follows:

$$\xi = \frac{\xi_L}{1 + \xi_L(1 - \bar{A}/\bar{B})},\quad \xi_L = \tilde{V}_1^0(0)/\tilde{V}_2^* \tag{6}$$

where $\tilde{V}_1^0(0)$ is the molar volume of the equilibrium liquid solvent (tracer) at 0 K, $(\bar{B}/\bar{A})$ is the aspect ratio of the solvent molecule and $\tilde{V}_2^*$ is the critical free volume per mole of jumping units required for a jump. E^* is estimated from the solubility parameters δ_1 and δ_2 of penetrant and polymer using a "universal" plot ([16, Fig. 1]), which we fitted by:

$$\log_{10}(E^*/\mathrm{cal\ mol}^{-1}) = 0.8988 \ln\{\log(\delta_1 - \delta_2)^2 \tilde{V}_1^0/\mathrm{cal\ mol}^{-1}\} + 2.8377 \tag{7}$$

Methods have been given [16] for a priori estimates of all parameter values required for evaluation of the above

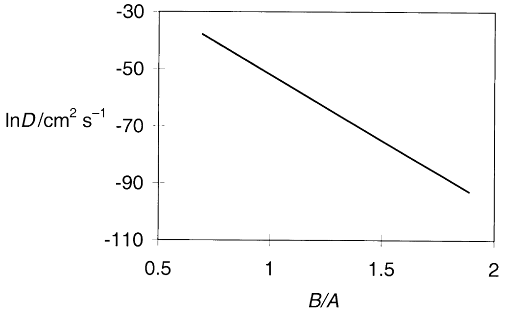

Fig. 1. Sensitivity of diffusion coefficients predicted by free-volume theory to the aspect ratio, ($\bar{B}/\bar{A}$) (all other parameters are listed in Table 1).

expressions, and these procedures were followed here, except as discussed below.

The parameters used for the prediction of the diffusion coefficients of the tracer dyes in PMMA at $w_\mathrm{p} = 1$ are listed in Table 1. The value used for $\bar{D}_0$ is from MMA data, and is certainly larger than the "true" value, but this does not change the central conclusions. The solubility parameter for penetrant was obtained using additivity rules and the Fedors parameters for cohesive energy and molar volume group contributions [20].

3. Comparisons of free-volume theory with experimental data

Now, it will be seen that the free-volume model greatly underestimates the diffusion coefficient in the temperature range studied, and so where there was some flexibility in the value of a particular parameter, the choice was made in a way that would give better agreement with experiment, i.e. in a way that would give a larger diffusion coefficient. In particular, the value of D is sensitive to that of the aspect ratio ($\bar{B}/\bar{A}$). In choosing this value, there are some uncertainties. It can be estimated semi-empirically using software developed and made available by Jurs and co-workers [21]. However, this is a complex calculation. In the present case, a sensitivity analysis was carried out over a reasonable range of ($\bar{B}/\bar{A}$), as shown in Fig. 1 (with all other parameters being those in Table 1). The value of D calculated with any reasonable value of ($\bar{B}/\bar{A}$) was always orders of magnitude less than experiment; a value of the aspect ratio of 0.9 was chosen, which lies within an appropriate range for penetrants used here, and gives a larger value for D.

Fig. 2 shows, as an Arrhenius plot, the comparison of experimental diffusion coefficients with those predicted by free-volume theory. The free-volume predictions are many orders of magnitude lower than any experimentally observed value.

It is apparent that the activation energy predicted by free-volume theory for this glassy system is much too big: about a factor of 2 greater than observed experimentally ($\sim$125 kJ mol^{-1}). The discrepancy is far greater than the uncertainties in the experimental activation energy.

The calculations show strong sensitivities to the following parameters: ($\bar{B}/\bar{A}$), $\tilde{V}_1^0(0)$, and E^*. Now, in all cases, the diffusion coefficients were predicted to decrease, and activation energies increase, as the values of these parameters increased. Since the values of the parameters chosen in Table 1 were towards the minimum values of a reasonable range, it can be seen that any reasonable variations in the values of these parameters will thus decrease the diffusion coefficients and increase the activation energy. Since the predicted diffusion coefficients are already much lower than the (extrapolated) experimental values, and the activation energy much larger, it appears that the agreement between prediction and experiment is poor, regardless of the choice of these parameters.

It should be noted that a reasonable fit to the diffusion data could be obtained using free-volume theory by allowing a number of the parameters to vary. This curve-fitting approach might be useful for interpolation or extrapolation of data for a particular system; however, here our objective is to test the predictive capability of free-volume theory.

It is postulated here that the reason for the poor agreement with the predictions of free-volume theory is that the fundamental precepts of free-volume theory are inapplicable to penetrant diffusion in a glassy polymer. There is strong evidence from simulations [1,22–25] that diffusion in glassy systems occurs through the penetrant, sitting in a polymer pocket, occasionally hopping to another pocket through a neck in the polymer opened by a random fluctuation.

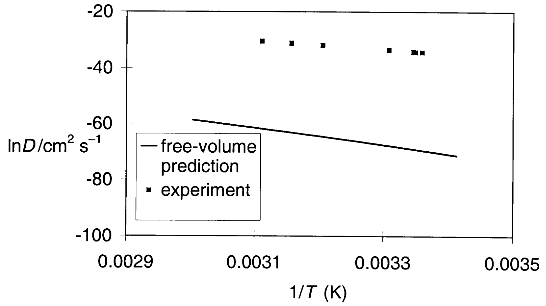

Fig. 2. Arrhenius plot comparing experimental diffusion coefficients with those predicted by free-volume theory (parameters listed in Table 1).

4. "Typical jump" model

4.1. Theory

The "typical jump" model of Gray-Weale et al. [17], is explicitly based on the above-mentioned hopping mechanism. It uses transition state theory to predict diffusion coefficients of small penetrants in glassy matrices, based on the interaction potentials of the polymer and penetrant, and the elastic properties of the polymer matrix. The model successfully predicts (within an order of magnitude) the diffusion coefficients of simple gases, small hydrocarbons and alcohols in glassy poly(vinyl chloride) over a wide range of values of experimental diffusion coefficients. However, the model is largely untested for other, more structurally complicated systems such as PMMA (which has a number of different side groups), the system studied here. Of the two variants of the model, the linear elastic solid model gave the best agreement with experiment for the larger penetrants, and will be used in the following comparisons.

The details of the model are described by Gray-Weale et al. The model calculates a rate coefficient k_{jump} for a typical jump by transition state theory in the usual manner [26]:

$$k_{\text{jump}} = \frac{\mathrm{k_B}T}{h}\frac{Q^{\dagger}}{Q}\exp\left(\frac{-E_0}{\mathrm{k_B}T}\right) \tag{8}$$

where $Q^{\dagger}/Q$ is the ratio of the partition function of the transition state to the reactant state, E_0 is the critical energy, and $\mathrm{k_B}$ is Boltzmann's constant. The diffusion coefficient for a jump is calculated from the rate coefficient by assuming only typical jumps (of length L) take place:

$$D = \frac{1}{6}k_{\text{jump}}L^2 \tag{9}$$

where D is the calculated diffusion coefficient. The jump length is calculated by assuming that a typical jump is from one cavity to another, through a neck past part of a polymer chain, which was shown (by transition state theory simulations) to be a polymer side group. The jump length is measured from the centre of one cavity to the next, and so the diameter of the cavity needs to be included, such that the jump length is equal to the Lennard-Jones diameter of the side group plus the diameter of the cavity:

$$L = L_{\mathrm{n}} + 2r_{\mathrm{i}}^{\mathrm{RS}} \tag{10}$$

Here L_{n} ($=\sigma$ (side group)) is the Lennard-Jones diameter of the side group, and $r_{\mathrm{i}}^{\mathrm{RS}}$ is the radius of the reactant cavity. It is assumed that only a few modes are important in the determination of the ratio of the partition functions, such that $Q^{\dagger}/Q$ can be written:

$$\frac{Q^{\dagger}}{Q} = \frac{q_{\mathrm{pe}}^{\dagger}q_{\mathrm{LJ}}^{\dagger}q_{\mathrm{def}}^{\dagger}}{q_{\mathrm{pe}}q_{\mathrm{LJ}}q_{\mathrm{def}}} \tag{11}$$

where q_{pe} is the partition function for the penetrant's internal motions, q_{LJ} is the partition function for the motion of the penetrant in the Lennard-Jones force field of the polymer, and q_{def} is the partition function for the deformation of the polymer.

In the theory, the penetrant is treated as a united atom, so $q_{\mathrm{pe}} = q_{\mathrm{pe}}^{\dagger}$. The ratio $q_{\mathrm{def}}/q_{\mathrm{def}}^{\dagger}$ is approximated as unity (although it may be slightly less). The other partition functions are found from the translational motions of the penetrant in the force field of the polymer, via the harmonic approximation. The Lennard-Jones field is treated as a sum of potentials for each neighbouring polymer side group involved in the jump:

$$V_{\mathrm{LJ}} = 4\varepsilon\left[\left(\frac{\sigma}{|\mathbf{r}-\mathbf{r}_{\mathrm{sg}}|}\right)^{12} - \left(\frac{\sigma}{|\mathbf{r}-\mathbf{r}_{\mathrm{sg}}|}\right)^{6}\right] \tag{12}$$

where ε is the Lennard-Jones well depth, σ is the Lennard-Jones diameter of the penetrant, $\mathbf{r}$ is the position of the penetrant, and $\mathbf{r}_{\mathrm{sg}}$ is the location of the side group. It is assumed in the present study (in the absence of better estimates) that the number of side groups is the same as in the study of Gray-Weale et al. That is, the transition state has three groups arranged trigonally and the reactant state has four groups arranged tetrahedrally. The force constants are taken as the second derivatives of the potential function at its minimum. The corresponding (quantum) vibrational partition function is then found in the usual way.

The overall potential energies in the reactant and transition states are given by the sum of the deformation potentials (V_{def}) and the Lennard-Jones potentials (V_{LJ}) of the penetrant in the neck or cavity. The difference between the energies at the minima of these functions (with respect to distance, r) gives the critical energy:

$$E_0 = \min(V^{\mathrm{TS}}) - \min(V^{\mathrm{RS}}) \tag{13}$$

The linear elastic solid model of Gray-Weale et al. assumes that the polymer behaves like a linear elastic solid in the vicinity of the deformation required to form the neck, with the same material constants as the bulk (macroscopic) solid. The quantities necessary to determine the critical energy are the energy required to form the neck in the transition state, and the energy required to expand the reactant cavity in the reactant state. The expressions for the deformation potentials (V_{def}, the energies required to deform the cavity or neck to a radius r_{i}) are:

$$V_{\mathrm{def}}^{\mathrm{RS}} = 8\pi\mu r_{\mathrm{i}}^{\mathrm{RS}}(r_{\mathrm{i}} - r_{\mathrm{i}}^{\mathrm{RS}})^2 \tag{14}$$

$$V_{\mathrm{def}}^{\mathrm{TS}} = 2\pi\mu L_{\mathrm{n}}(r_{\mathrm{i}} - r_{\mathrm{i}}^{\mathrm{TS}})^2 \tag{15}$$

where the superscripts RS and TS refer to the reactant state and transition state, respectively, $r_{\mathrm{i}}^{\mathrm{TS}}$ is the radius of the transition state neck, and μ is one of the Lamé elastic constants, which is equal to the shear modulus of the polymer, and is defined by:

$$\mu = \frac{E}{2(1+\nu)} \tag{16}$$

Here E is Young's modulus, and ν is Poisson's ratio for the polymer. Young's modulus, Poisson's ratio, and the isothermal compressibility (κ) are related by:

$$E = 3\kappa^{-1}(1-2\nu) \tag{17}$$

The Lennard-Jones potentials representing the interaction between the penetrant and the polymer are calculated for the penetrant in a neck or cavity of radius r, and are of the

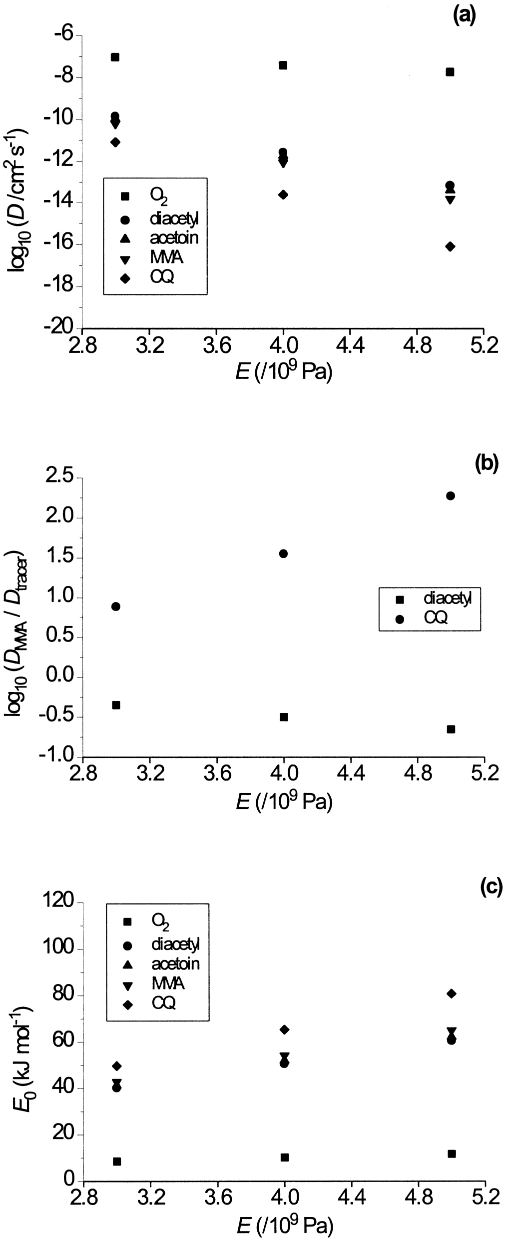

Fig. 3. Sensitivity of diffusion coefficients predicted from the typical-jump model to changes in Young's modulus (E) for PMMA: (a) absolute diffusion coefficients; (b) ratios of predicted diffusion coefficients; and (c) critical energies. Note that μ is proportional to E, so changes in μ are proportional to changes in E.

following form:

$$V_{\mathrm{LJ}}(r) = 4n\varepsilon\left[\left(\frac{\sigma}{r'}\right)^{12} - \left(\frac{\sigma}{r'}\right)^{6}\right] \tag{18}$$

where n is the number of neighbouring polymer side groups (3 for the transition state, and 4 for the reactant state), and $r' = r + (1/2)\sigma_{\mathrm{sg}}$ (σ_{sg} is the Lennard-Jones diameter of the side group) is the distance between the side group and penetrant "atoms" (noting that the side and reactant groups are treated as united atoms).

The values for σ and ε are calculated using by standard combination rules for Lennard-Jones interactions:

$$\sigma = \tfrac{1}{2}(\sigma_{\mathrm{A}} + \sigma_{\mathrm{B}}) \tag{19}$$

$$\varepsilon = \sqrt{\varepsilon_{\mathrm{A}}\varepsilon_{\mathrm{B}}} \tag{20}$$

where A and B denote the two interacting groups.

Thus, given ε and σ for the side groups and penetrant, the deformation potentials, and by finding the minima of the potential functions for the transition and reactant states, the critical energy for a typical jump can be calculated. The rate coefficient for a typical jump can then be calculated, and the diffusion coefficient obtained using Eq. (9).

4.2. Estimation of parameters

The diffusion coefficients were calculated in the following manner:

- The deformation potentials were calculated using Eqs. (14), (15) and (18).
- The minima of these functions were used to calculate E_0 using Eq. (13).
- The force constants for these degrees of freedom were calculated from the second derivatives of the potential functions given by Eq. (12).
- The vibrational partition functions for each degree of freedom of each of the penetrants were evaluated.
- The product of these partition functions for both the transition and reactant states were used to calculate $(Q^{\dagger}/Q)$.
- The rate coefficients were then given by the transition state formula in Eq. (8), using the above values for E_0 and $(Q^{\dagger}/Q)$.
- The diffusion coefficients were then calculated using Eq. (9) and using the value from Eq. (10) for the jump length.

The parameters required to generate diffusion coefficients are the elastic parameters for PMMA as a function of composition and temperature (in particular, μ, one of the Lamé elastic constants, which is equal to the shear modulus of the polymer), the Lennard-Jones parameters for the side groups ($\varepsilon_{\mathrm{sg}}$, σ_{sg}), and the radii of the reactant cavity and the transition state neck.

These parameters were estimated as follows. The value of μ for the pure polymer is taken as [27] 1700 MPa at 25°C (and the temperature dependence estimated by the change in κ, and by the use of Eqs. (16) and (17)), the radii of the reactant cavity and transition state neck were approximated by the values used by Gray-Weale et al. (giving reasonable agreement with experiment), and the Lennard-Jones parameters for the side groups and penetrants estimated as described below. Poisson's ratio was calculated by combining the results of Eqs. (16) and (17), with the known values for κ and μ at 25°C. The value so obtained is 0.314, in reasonable accord with the typical values (0.32–0.36) for "fat" polymer chains (those with large side groups) in glassy

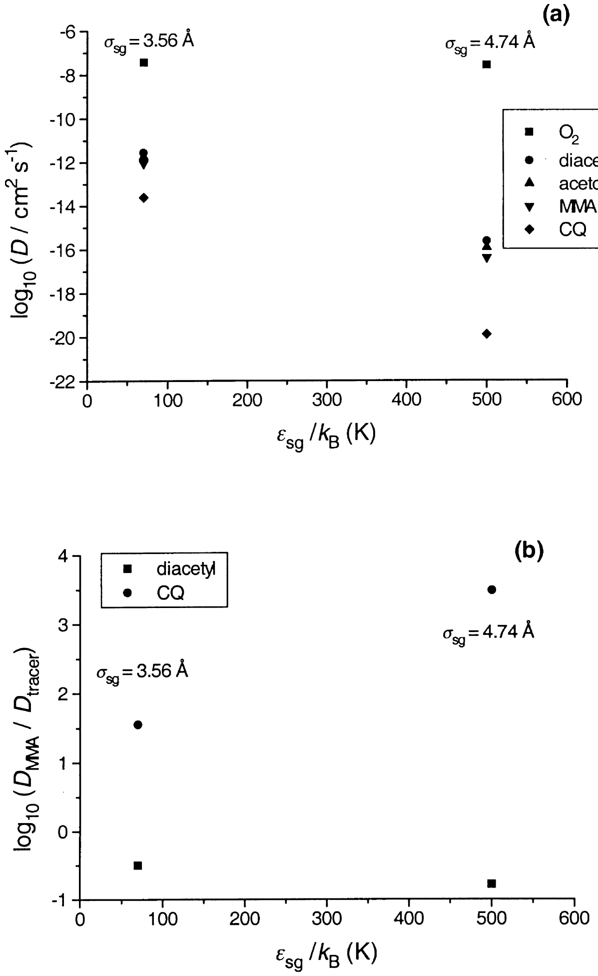

Fig. 4. Sensitivity of diffusion coefficients predicted from the typical-jump model to variations in the well depth for the side groups: (a) absolute predicted diffusion coefficients and (b) ratios of predicted diffusion coefficient. $T = 50°C$. Note that the Lennard-Jones diameters of the side groups are different in each case, since these values represent the minimum and maximum side group interactions, corresponding to the side groups CH_3 (minimum) and CO_2CH_3 (maximum).

polymer matrices [28]. It is worth noting that ν is usually temperature-dependent, but this temperature dependence is weak for temperatures more than 20°C below T_g [28]. Poisson's ratio rapidly approaches 0.5 from below at temperatures above this point. However, all calculations here are at least 40°C below the glass transition, and thus ν can be reasonably well approximated as constant in this interval. The maximum value in this interval is likely to be $\nu = 0.36$ (the upper limit for "fat" polymer chains). The effects of this variation are shown at the lower limit for E in Fig. 3.

The number of side groups (n) in the transition and reactant states were taken, in the absence of better evidence, as those of Gray-Weale et al., i.e. 3 and 4, respectively. The radii of the transition state neck and the reactant cavity were varied about the values used by Gray-Weale et al. for polypropylene, in order to test the sensitivity to these parameters in the current system. The values giving the best agreement with experiment will be used for the comparison with experiment. The Lennard-Jones parameters were calculated according to the methods described in Gilbert and Smith [26], with the exception of the maximum well depth for camphorquinone. The Lennard-Jones diameters for the molecules were calculated by the summation of individual volume contributions (V_i) from the component atoms (or groups), according to the expression [29]:

$$\sigma_{LJ} = 1.45 \sum_{i}^{N} V_i \tag{21}$$

where N is the number of individual volume contributions. The well depths for the molecules were estimated from their boiling points (T_b), according to the expression [29]:

$$\varepsilon/k_B = 1.21 T_b \tag{22}$$

It is uncertain which side groups are involved in the jumping process, since there are no transition state simulations for this system (which is more structurally complicated than the systems studied by Greenfield and Theodorou and by Gray-Weale et al., viz. poly(vinyl chloride) and polypropylene). The most likely candidates are CH_3, OCH_3, or CO_2CH_3. The methyl group may be the most likely of these, since it is the smallest, and thus gives the lowest critical energy. However, a likely scenario is that the penetrant must jump past a mixture of these side groups. Thus, for the side groups involved in the jump, estimates of the diffusion coefficients have been made for the two extreme cases (CH_3, and CO_2CH_3). The "true" value is likely to lie between these two extremes. The well depth for CH_3 was taken from the study of Gray-Weale et al., and estimated for the case of CO_2CH_3 as 500 K. The errors in the estimates of the well depths for the side groups are unlikely to make a large difference to the results, since the calculations are relatively insensitive to this parameter (see Fig. 4).

The individual volume contributions (and resulting σ values) and melting points (and corresponding ε values) for oxygen, diacetyl, acetoin (the photoproduct produced in the photoreaction of diacetyl), MMA and camphorquinone are listed in Table 2. Note that the ε value for camphorquinone is calculated from the melting point (T_m) (since the dye undergoes sublimation), rather than the boiling point, by [29]

$$\varepsilon/k_B = 1.92 T_m \tag{23}$$

The predicted diffusion coefficients were generated using a variety of input parameters (generally with greater than the expected maximum deviations), in order to test the sensitivity of the diffusion coefficients predicted by the model to these parameters. The parameters varied were the Lamé elastic constant (μ), the reactant cavity and transition state neck radii (r_i^{RS}, r_i^{TS}), and the Lennard-Jones parameters for the penetrants and the side groups. The parameters that gave

Table 2
Lennard-Jones parameters for the small penetrants considered in this study

Molecule	Oxygen	Diacetyl ($CH_3COCOCH_3$)	Acetoin ($CH_3COC(OH)HCH_3$)
T_b (K)	90.2	361	416.5
ε/k_B (K)	118[a]	436.8	503.4
V_1 (Å^3)	Not used	4×8.9 (carbons)	4×8.9 (carbons)
V_2 (Å^3)		6×2.2 (hydrogens)	8×2.2 (hydrogens)
V_3 (Å^3)		2×4.5 (double-bonded oxygens)	1×4.5 (double-bonded oxygen)
V_4 (Å^3)			1×6.0 (single-bonded oxygen)
$\sum(V_i)$ (Å^3)	Not used	57.8	59.3
σ (Å)	(3.46[a])	5.61	5.65
Molecule Formula	Methyl methacrylate $CH_2C(CH_3)CO_2CH_3$	Camphorquinone $C_{10}H_{14}O_2$	
T_b (K)	373	473–476[b]	
ε/k_B (K)	451.3	908–914	
V_1 (Å^3)	5×8.9 (carbons)	10×8.9 (carbons)	
V_2 (Å^3)	8×2.2 (hydrogens)	14×2.2 (hydrogens)	
V_3 (Å^3)	1×4.5 (double-bonded oxygen)	2×4.5 (double-bonded oxygens)	
V_4 (Å^3)	1×5.5 (single-bonded oxygen)	-9.0 (6-membered ring)	
$\sum(V_i)$ (Å^3)	72.1	119.8	
σ (Å)	6.04 (5.85[c])	7.15	

[a] The parameters for oxygen are from experiment [29].

[b] The ε value for camphorquinone is calculated from the melting point, rather than the boiling point, using Eq. (20).

[c] The more commonly used value for much of the polymer kinetics work.

the best-fit to the experimental data for camphorquinone and diacetyl are listed in Table 3.

4.3. Results and sensitivities

Strong sensitivities to variations in input parameters were shown for variations in the Lennard-Jones diameters of the penetrants and side groups, the elastic constant of the polymer, and the radii of the reactant cavity and transition state neck. The predicted diffusion coefficients were relatively insensitive to variations in the Lennard-Jones well depths for the side groups and penetrants. The apparently high sensitivity of the predicted diffusion coefficients to the well depths for the side groups in Fig. 4 is primarily due to the fact that this plot represents the maximum predicted change in behaviour, based on changing from the smallest (least polar) side group to the largest (most polar) side group. The plot thus represents the sensitivity to changes in both the well depth and the Lennard-Jones diameter of the side group, and should not be interpreted as the change due solely to changes in the well depth of the side group.

Table 3
Parameters used for the scaling of tracer dye to methyl methacrylate diffusion coefficients at 50°C, using the theory of Gray-Weale et al. For the rows containing more than one value, the numbers are for each penetrant, as follows: molecular oxygen, diacetyl, acetoin, methyl methacrylate, camphorquinone

E (Pa)	4×10^9
ν	0.3139
T (K)	323
r_i^{RS} (Å)	2.6
r_i^{TS} (Å)	1.1
σ_{pen} (Å)	3.46, 5.61, 5.65, 5.85, 7.15
σ_{sg} (Å)	3.56
ε_{pen}/k_B (K)	118, 436.8, 503.4, 451.3, 1060
ε_{sg}/k_B (K)	70
m (a.m.u.)	32, 86.09, 88.11, 100.12, 166.2

The ratios of the predicted diffusion coefficients were also compared as a function of variations in input parameters. It was found that the ratios of the predicted diffusion coefficients (MMA to camphorquinone) were relatively insensitive to the well depths for the side groups and penetrants, and were relatively sensitive to the elastic parameters of the matrix, the Lennard-Jones diameters of the side groups and penetrants, and the radii of the reactant cavity and the transition state neck. For the case of the ratio of predicted diffusion coefficients between MMA and diacetyl, the same trends were observed. However, the ratios of predicted diffusion coefficients for MMA to diacetyl were generally much less sensitive to variations in input parameters, due to the similarity in Lennard-Jones parameters for MMA and diacetyl, and the desired scaling is reasonably well approximated even with variations in the best-fit parameters.

The strong sensitivities of the predicted diffusion coefficients, their ratios, and the effective activation energies to the radii of the reactant cavity and the transition state neck, are due primarily to the nature of the elastic deformation potentials. The deformation potentials dominate the behaviour

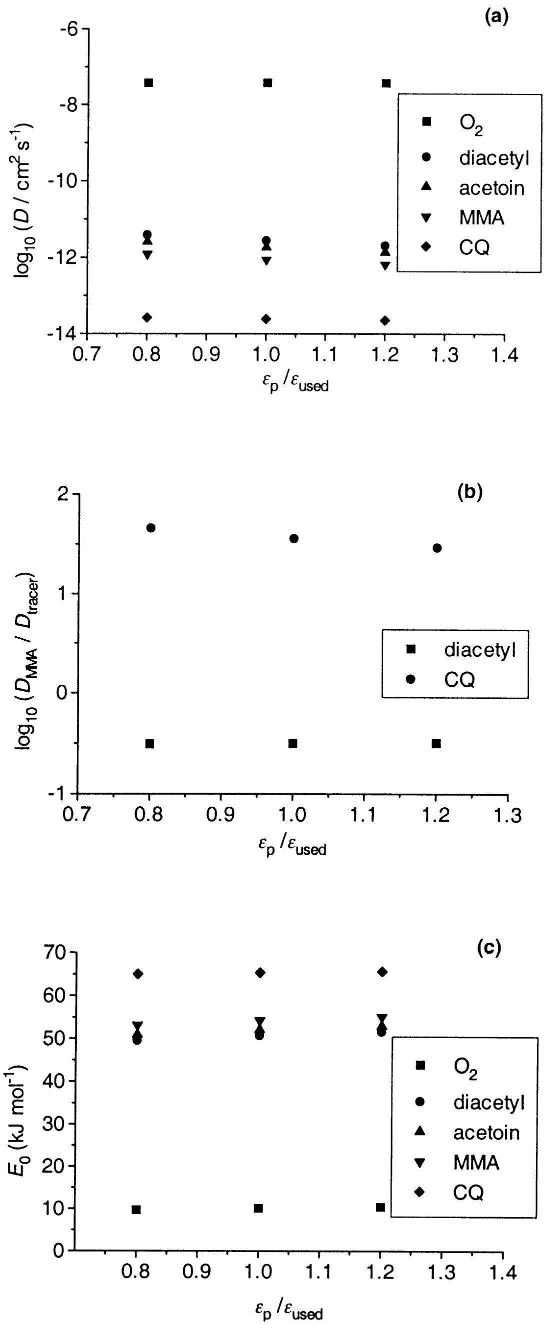

Fig. 5. Sensitivity of diffusion coefficients predicted from the typical-jump model to variations in the well depth for the penetrants: (a) absolute predicted diffusion coefficients; (b) ratios of predicted diffusion coefficients; and (c) critical energies. $T = 50°\text{C}$, $\varepsilon_{\text{used}}$ is the value of ε_p shown in Table 3.

of the system, and for the reactant and transition states are strongly dependent on r_i^{RS} and r_i^{TS}, respectively. Thus, the predicted critical energies and diffusion coefficients are strongly dependent on these quantities.

The sensitivities of the diffusion coefficients (and their ratios) for molecular oxygen, diacetyl, MMA, acetoin, and camphorquinone to variations in the input parameters are shown in Figs. 3–7.

The change in the elastic parameters due to temperature or conversion was estimated by combining Eq. (16) and (17), and noting that μ is proportional to κ^{-1}. Thus, the change in μ is inversely proportional to the change in κ.

The strategy used to find the input parameters in Table 3 was to use the known input parameters without variation, and use the radii of the reactant cavity and transition state neck as variables. The aim was to attempt to match both the absolute values of the diffusion coefficients at 50°C, and approximately predict the activation energies for these processes, where known. The two cases where activation energies were available were for O_2 (30 kJ mol^{-1} [30]) and camphorquinone (~125 kJ mol^{-1} [15]). Note that the activation energy for diffusion of oxygen was measured over very small distance scales, and the diffusion in such a case is almost certainly anomalous (and a large distribution of apparent diffusion coefficients were required to fit the data). The "true" activation energy for the diffusion of oxygen in the system therefore may be different from that reported, and should be taken as an approximation only. A possible difference between the systems being compared is that the O_2 diffusion measurements were at very low temperatures (≈ 100 K), whereas the predictions are centred around 323 K.

The predicted activation energies that were used for comparison were determined by numerical differentation of $\ln D$ as a function of T^{-1}. The critical energies predicted by the program are of course similar to, but significantly less than, the activation energies (for reasons that are well understood [26]: the activation energy is the slope of an Arrhenius plot but the critical energy is a physical parameter giving the minimum energy for the process).

4.4. Comparison with experiment

The best-fit parameters are listed in Table 3. A reasonable set of input parameters could not be found that could simultaneously match both the activation energies and diffusion coefficients. The discrepancy cannot arise simply because the data needed to be extrapolated to $w_p = 1$. The observed activation energy for diffusion of camphorquinone in PMMA beyond the glass transition is independent of conversion (w_p), within the experimental uncertainty [15]. Additionally, the diffusion coefficients for several small tracer dyes in glassy polymers, when measured as a function of temperature [9], also showed approximately constant activation energies throughout the glassy regime. Note that the model predicts a significant non-linearity in this region (see Figs. 8 and 9), the primary origin for which is the change in the elastic parameters of the matrix with temperature; however, it could not be concluded that there is a contradiction between the experimental observations and prediction, because the extent of the predicted non-linearity was probably too small to be observed experimentally.

It could be argued that the theoretical basis for the typical-jump model for the prediction of diffusion coefficients

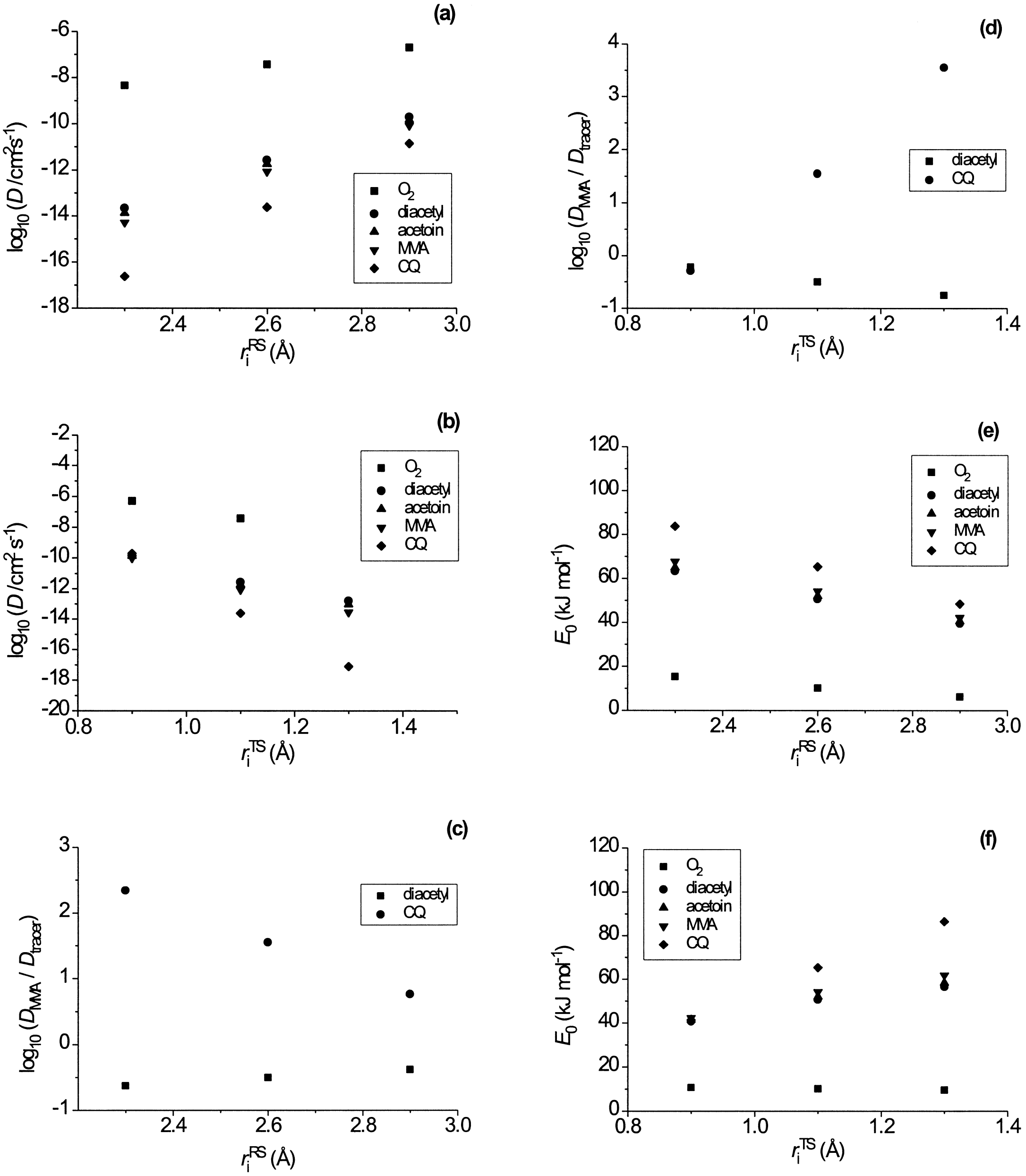

Fig. 6. Variations in diffusion coefficients predicted from the typical-jump model: (a) with varying r_i^{RS}, (b) varying r_i^{TS}; ratios of predicted diffusion coefficients with: (c) varying r_i^{RS}, (d) varying r_i^{TS}; and critical energies with: (e) varying r_i^{RS}, (f) varying r_i^{TS}. The missing point for oxygen on plot (b) is due to the neck being large with respect to the penetrant, leading to problems finding the minimum of the potential function.

may not be applicable in the presence of added diluent (which was always the case in this study): addition of diluent may plasticize the matrix, and free volume considerations may become necessary. However, the relatively small change in measured D with w_p above $w_p \sim 0.85$ showed that the added diluent does not change the dominant mechanism for diffusion in glassy polymers, and thus the typical jump model should still be applicable.

Another experimental observation [15] is that the ratio of diffusion coefficients for the tracer dye and its photoproduct does not appear to change significantly with w_p within (the rather large) experimental uncertainty. If the elastic parameters of the matrix are assumed to change with composition, then the predicted diffusion coefficients will also change with composition, which is contrary to the experimental observations. Fig. 3 shows the predicted effects of changing composition on the diffusion coefficients and their ratios, compared with the experimental observations. As can be clearly observed, the qualitative prediction of a large change in scaling ratio for camphorquinone is very different from experiment. Incidentally, the model predicts changing activation energies as a function of composition, again because of the changing elastic properties of the matrix. This prediction also contradicts the

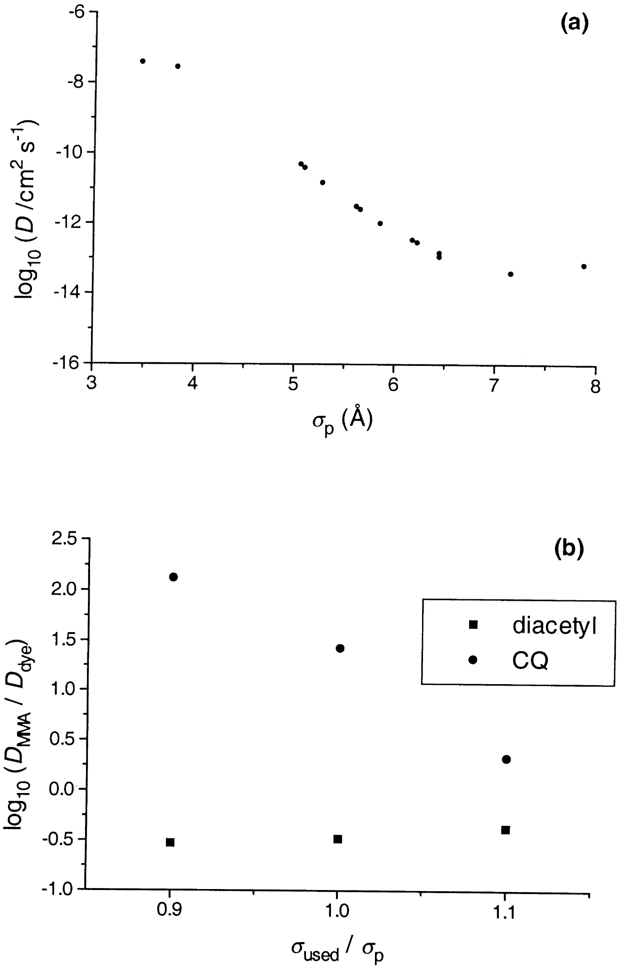

Fig. 7. Sensitivity of diffusion coefficients predicted from the typical-jump model to 10% variations (the maximum likely uncertainty [29]) in Lennard-Jones radii of penetrants: (a) absolute predicted diffusion coefficients; and (b) ratios of predicted diffusion coefficients. A constant value for the well depth of 400 K was used for each point. Note that the predicted diffusion coefficients scale approximately linearly with σ_p in the centre of the plot (as may be expected [17,29]), but deviate from linearity at either extreme. The observed non-linearity is probably due to the penetrant being either substantially smaller or larger than the reactant cavity.

experimental observation that the activation energy is independent of w_p. The values of these predictions at the glass transition could be calculated by assuming that the elastic parameters of the matrix were the same for added diluent as for increasing temperature (see Fig. 10). The elastic parameters at the glass transition (reached by adding diluent) could then be estimated as the same as the values at 120°C in Fig. 10. However, such an approach appears to be unnecessary for the scaling of diffusion coefficients, based on the experimental observation that the scaling appears to be approximately independent of w_p.

Although there are uncertainties in all of the input parameters for the prediction of diffusion coefficients by this theory, only two of the parameters could be considered freely adjustable (and even these are constrained). These parameters are the radii of the reactant cavity in the reactant state and the neck in the transition state. These values can be adjusted, but as described above, it was found that only either the absolute diffusion coefficients or the activation energies, not both simultaneously, could be accurately predicted using the model, despite variations in r_i^{RS} and r_i^{TS}.

An attempt was made to solve this problem by reducing the input value of Young's modulus (as a function of temperature) uniformly by up to 30%, such that reasonable estimates of both the activation energies and diffusion coefficients could be simultaneously obtained. However, this strategy was not successful in obtaining the desired results. Attempts to improve the fit to the experimental observations by changing the parameters for the side groups failed disastrously. Since the methyl group used for the predictions above is the smallest candidate for the possible side group, predictions based on larger side groups (see Fig. 4) gave much larger activation energies than for the case of the methyl groups. This is due to the strong dependence of the predicted values on the Lennard-Jones diameters of both the penetrants and side groups. Since the predicted activation energies are already much too large compared with experiment, the fit to the experimental observations was actually much worse than for the case using methyl side groups. Thus, the final parameter set used in Table 3 assumes that the side groups are methyl groups, although this may not adequately model the physics of the real system.

The activation energies for the diffusion coefficients can be forced to fit the experimental data by selection of appropriate values of r_i^{RS} and r_i^{TS}. However, the diffusion coefficients are then predicted to be too large. A further adjustment could be made for the case of oxygen (and probably the other species) by reducing the Lennard-Jones diameter of the penetrant. This leads to lower predicted activation energies, and may be a reasonable adjustment considering that the transition state neck may for the case of PMMA have a significantly different geometry from that assumed in the model. However, the absolute value of the diffusion coefficient is then again too large. Thus, there appear to be no reasonable adjustments that can be made to input parameters that allow simultaneous prediction of the activation energies and absolute diffusion coefficients for the case of glassy PMMA.

It was observed experimentally [15] that the ratio of diffusion coefficients for diacetyl to acetoin (the photoproduct of diacetyl) was approximately a factor of 4, and apparently independent of conversion. The predicted ratio of diffusion coefficients using the model of Gray-Weale et al. is ~1.5, as shown in Fig. 11. This ratio is relatively insensitive to variations in input parameters (since the Lennard-Jones parameters for the two species are very similar). Thus the model is unable to predict the large difference observed between the diffusion coefficients of diacetyl and acetoin. This is probably due to the model underestimating the attractive potentials that may form between the penetrant

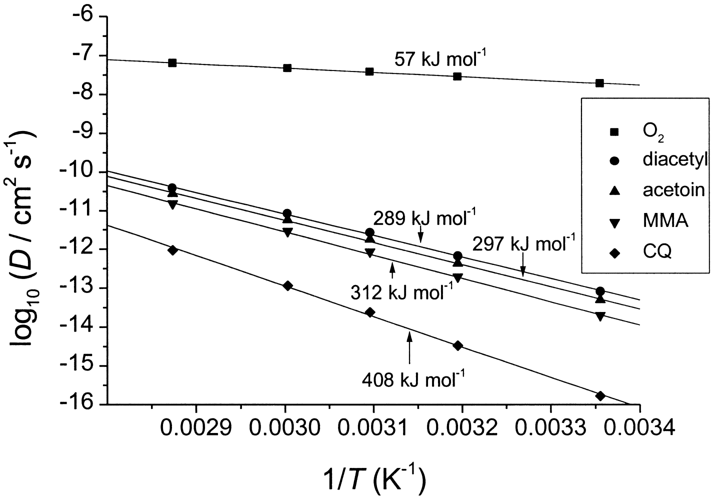

Fig. 8. Arrhenius plot and predicted apparent activation energies, calculated from $-\partial(\ln D)/\partial(1/T)$, for various penetrants in glassy PMMA. The plots are actually slightly curved, not linear. The purpose is to illustrate the apparent activation energies, based on both the critical energy, and changes in the matrix. The parameters used in the calculations are listed in Table 3.

and the polymer matrix. On this basis, it is assumed that it is likely that the model will predict diffusion coefficients that are too fast for highly polar species in matrices containing polar groups.

4.5. Limitations of the model

There are several possible reasons that the model may fail in this system (assuming that the fundamental precepts of the model are appropriate, as suggested by MD simulations). These include assumptions or calculations that may be questionable, and/or breakdown of the model under some conditions. Questionable assumptions or calculations include the treatment of the penetrants as hard spheres, and poor estimation of elastic constants for the polymer matrix. Breakdown of the treatment may occur due to deviations from linear elastic behaviour for the larger penetrants. Certainly for large linear penetrants, the deviations from sphericity are likely to be significant, and diffusion is likely to take place by motion in the direction of shortest cross-section. It is assumed here that the penetrants studied do not deviate sufficiently from an approximate sphere to make a large difference to the predictions of the model. However, this assumption may be incorrect.

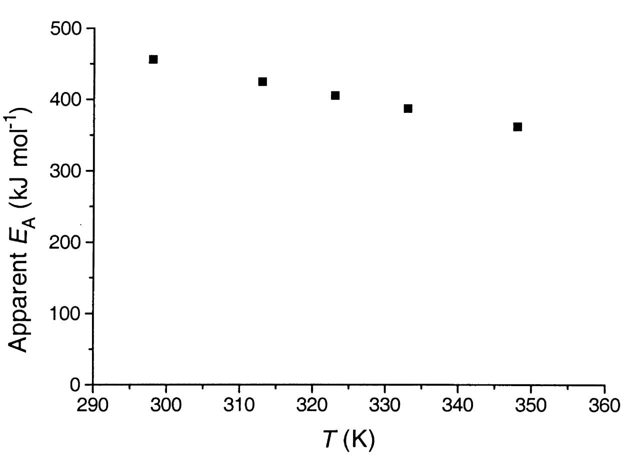

Fig. 9. Apparent activation energy as a function of temperature for camphorquinone, using the parameters from Fig. 8, and calculated from $-\partial(\ln D)/\partial(1/T)$.

For the set of parameters in Table 3, deviations from linearity of the elastic properties of the matrix may be significant. In particular, the Lennard-Jones radius of camphorquinone is much larger than the unperturbed radius of the reactant cavity. In this case, the linear elastic treatment may no longer be valid, and modifications of the treatment, such as modifications for 2nd-order corrections, may be necessary.

From the observed discrepancies, it appears likely that the model does not completely capture the essential physics responsible for diffusion of small penetrants (larger than those previously studied) of this size range in glassy polymers, particularly in PMMA, which is a more complicated system than those previously examined with the model [17]. It may be the case that the model may only strictly apply for smaller penetrants.

5. Conclusions

Two models (the free-volume approach of Vrentas et al., and the “typical jump” model of Gray-Weale et al.) for the diffusion of small penetrants in polymeric matrices were used to predict diffusion coefficients (and their associated activation energies) for several small molecules in amorphous glassy PMMA. The predictions of the two models for diffusion of small penetrants in polymeric matrices

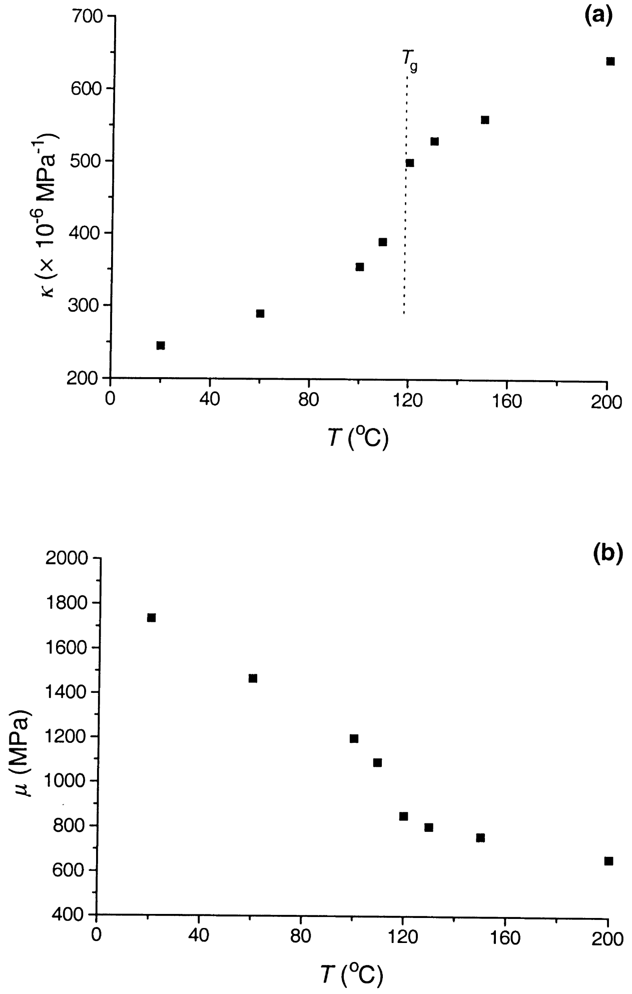

Fig. 10. Variation in: (a) isothermal compressibility (κ) with temperature for PMMA [27]; and (b) corresponding variation in μ with temperature (calculated assuming a constant value of ν).

were both found to give poor agreement with experimental observations of the diffusion of camphorquinone and diacetyl in glassy PMMA as measured by forced-Rayleigh scattering.

The free-volume approach predicts diffusion coefficients that are much too low (in the temperature range studied) when sensible parameter values were used; the predicted activation energies are much higher than experiment. It is considered likely that the failure of the model to reliably predict diffusion coefficients and associated activation energies in this system is due to the underlying mechanistic assumptions regarding the diffusion process, which are probably invalid in very glassy polymeric materials.

The “typical jump” model of Gray-Weale et al. is based on detailed transition state simulations of the diffusion process of small penetrants in glassy polymers, and thus avoids the mechanistic assumptions of free-volume theory that may be invalid in a glassy system. Although the theory of Gray-Weale et al. successfully predicts [17] diffusion coefficients of simple gases, small hydrocarbons and alcohols in glassy poly(vinyl chloride) over a wide range of values of experimental diffusion coefficients, it could not be used to simultaneously give good agreement between prediction and experiment for both the diffusion coefficients and activation energies in the current system. This is probably due to both the model missing some, but not all, of the essential physics of the diffusion process in this system, and limitations of the applicability of the model to relatively simple systems. The likely causes of the failure of the model are underestimation of the attractive potentials which may form between the penetrant and the polymer matrix in these more polar penetrant/polymer combinations, the failure to accurately describe the relatively complex microstructure of the polymer near the opening “neck”, and/or breakdown of the model’s assumption of linear elastic deformation for the relatively large penetrants used in this study.

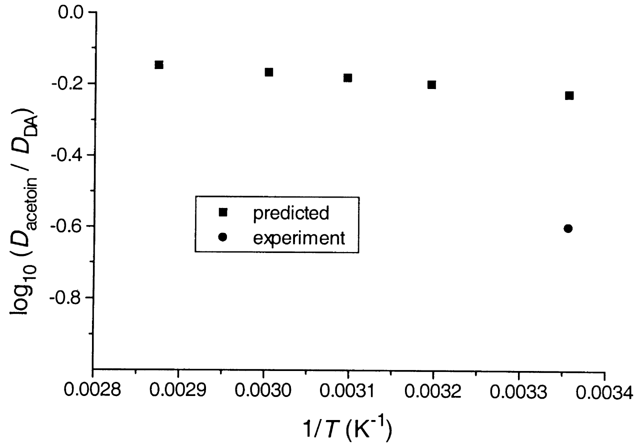

Fig. 11. Comparison of prediction (based on the typical jump model) versus experiment for the ratios of diffusion coefficients between diacetyl and acetoin in glassy PMMA. The predicted parameters were generated with the parameters in Table 3, and following the temperature dependence for the elastic parameters for the matrix indicated in Fig. 10.

Improved models for the diffusion of small penetrants in the glassy regime are an important step to the understanding of this process, and for the prediction and/or scaling of existing diffusion data to new systems. The failure of the existing models for this system suggests that further work is necessary from both a modelling point of view, and the measurement of reliable diffusion coefficients of small penetrants in a wider range of glassy systems.

Acknowledgements

The authors gratefully acknowledge the support of the Australian Research Council both for a Large Grant and through the establishment and support of the Key Centre for Polymer Colloids. Helpful interactions with Jeff Stubbs, Angus Gray-Weale and Narayan Ramesh are also much appreciated.

References

[1] Greenfield ML, Theodorou DN. Macromolecules 1998;31:7068.
[2] Gilbert RG. Emulsion polymerization: a mechanistic approach. London: Academic Press, 1995.
[3] Clay PA, Christie DI, Gilbert RG. Termination rate coefficients from molecular weight distributions. In: Matyjaszewski K, editor. Advances in free-radical polymerization, vol 685. Washington, DC: ACS, 1998. p. 104.
[4] Parker H-Y, Westmoreland DG, Chang H-R. Macromolecules 1996;29:5119.
[5] Gonález-Ortiz LJ, Asua JM. Macromolecules 1996;29:383.
[6] Gonález-Ortiz LJ, Asua JM. Macromolecules 1996;29:4520.
[7] Stubbs J, Karlsson O, Jonsson J, Sundberg E, Durant Y, Sundberg D. Colloids Surf A 1999;153:255–70.
[8] Sundberg EJ, Sundberg DC. J Appl Polym Sci 1993;47:1277.
[9] Ehlich D, Sillescu H. Macromolecules 1990;23:1600.
[10] Veniaminov AV, Sillescu H. Macromolecules 1999;32:1828.
[11] Zhang J, Wang CH. Macromolecules 1987;20:683.
[12] Geisel T, Zacherl A, Radons GZ. Physica B 1988;71:117.
[13] Chernikov A, Petrovichev B, Rogalsky A, Sagdeev R, Zaslavsku G. Phys Lett A 1990;144:127.
[14] Klafter J, Shlesinger MF, Zumofen G. Phys Today 1996;49:33.
[15] Tonge MP, Stubbs JM, Sundberg DC, Gilbert RG. Polymer 2000;41:3659.
[16] Vrentas JS, Vrentas CM. Eur Polym J 1998;34:797.
[17] Gray-Weale AA, Henchman RH, Gilbert RG, Greenfield ML, Theodorou DN. Macromolecules 1997;30:7296.
[18] Duda JL, Zielenski JM. Free-volume theory. In: Neogi P, editor. Diffusion in polymers, New York: Marcel Dekker, 1996. p. 143.
[19] Ferguson RD, von Meerwall E. J Polym Sci, Polym Phys Ed 1982;18:1285.
[20] van Krevelen DW. Properties of polymers. 3rd ed. Amsterdam: Elsevier, 1997.
[21] Jurs P. ADAPT: automated data analysis and pattern recognition toolkit, Department of Chemistry, Pennsylvania State University.
[22] Takeuchi H. J Chem Phys 1990;93:2062.
[23] Sok RM, Berendsen HJC, van Gunsteren WF. J Chem Phys 1992;96:4699.
[24] Müller-Plathe F, Rogers SC, van Gunsteren WF. J Chem Phys 1993;98:9895.
[25] Greenfield ML, Theodorou DN. Macromolecules 1993;26:5461.
[26] Gilbert RG, Smith SC. Theory of unimolecular and recombination reactions. Oxford and Cambridge, MA: Blackwell Scientific, 1990.
[27] Brandrup J, Immergut EH, Grulke EA. In: Brandrup J, Immergut EH, Grulke EA, editors. Polymer handbook, 4th ed. New York: Wiley, 1999.
[28] Bicerano J. Prediction of polymer properties. 2nd ed. New York: Marcel Dekker, 1996.
[29] Hirschfelder JO, Curtiss CF, Bird RB. Molecular theory of gases and liquids. New York: Wiley, 1964.
[30] Bazhin NM, Korolev VV, Mamaev AL, Bol'shakov BV. J Polym Sci: Part B: Polym Phys 1998;36:127.
[31] Waggoner RA, Blum FD, MacElroy JMD. Macromolecules 1993;26:6841.
[32] Haward RN. J Macromol Sci, Rev Macromol Chem C 1970;4:191.
[33] Griffiths MC, Strauch J, Monteiro MJ, Gilbert RG. Macromolecules 1998;31:7835.